JCB Article

# Espin cross-links cause the elongation of microvillus-type parallel actin bundles in vivo

**Patricia A. Loomis, Lili Zheng, Gabriella Sekerková, Benjarat Changyaleket, Enrico Mugnaini, and James R. Bartles**

Department of Cell and Molecular Biology, Feinberg School of Medicine, and Institute for Neuroscience, Northwestern University, Chicago, IL 60611

The espin actin-bundling proteins, which are the target of the jerker deafness mutation, caused a dramatic, concentration-dependent lengthening of LLC-PK1-CL4 cell microvilli and their parallel actin bundles. Espin level was also positively correlated with stereocilium length in hair cells. Villin, but not fascin or fimbrin, also produced noticeable lengthening. The espin COOH-terminal peptide, which contains the actin-bundling module, was necessary and sufficient for lengthening. Lengthening was blocked by 100 nM cytochalasin D. Espin cross-links slowed actin depolymerization in vitro less than twofold. Elimination of an actin monomer-binding WASP homology 2 domain and a profilin-binding proline-rich domain from espin did not decrease lengthening, but made it possible to demonstrate that actin incorporation was restricted to the microvillar tip and that bundles continued to undergo actin treadmilling at ~1.5 $s^{-1}$ during and after lengthening. Thus, through relatively subtle effects on actin polymerization/depolymerization reactions in a treadmilling parallel actin bundle, espin cross-links cause pronounced barbed-end elongation and, thereby, make a longer bundle without joining shorter modules.

## Introduction

At the core of microvilli and stereocilia is a parallel actin bundle (PAB) composed of actin filaments of uniform polarity cross-linked by actin-bundling proteins (DeRosier and Tilney, 2000). Because the plasma membrane of microvilli and stereocilia conforms to these PABs, the PABs appear to be molecular scaffolds that determine the dimensions of these fingerlike cellular protrusions.

PABs are known to contain different complements of actin-bundling proteins (Bartles, 2000), but little is known about what each contributes. For example, enterocyte brush border microvilli contain villin, fimbrin, and espin (Bartles, 2000), whereas hair cell stereocilia contain fimbrins (Tilney et al., 1989; Daudet and Lebart, 2002) and espin (Zheng et al., 2000). Consistent with the idea that each actin-bundling protein plays an important and specific role, mutations that impair or eliminate different actin-bundling proteins have distinguishable effects on PAB organization (Tilney et al., 1998; Ferrary et al., 1999; Zheng et al., 2000).

There are many indications that the lengths of microvilli and stereocilia, and hence their PAB scaffolds, are tightly regulated. Microvilli and stereocilia grow to markedly different lengths, even though both originate as microvillus-like precursors that emanate from electron-dense patches beneath the plasma membrane (DeRosier and Tilney, 2000). Microvillus length varies in a regular way among cell types, ranging from the 1–2-μm long, uniform brush border microvilli typical of enterocytes (Mooseker, 1985) to the 80-μm long microvilli of epithelial cells lining the human caput epididymidis (Pacini et al., 1980). Stereocilia also exhibit characteristic differences in length as a function of hair cell position in the inner ear. For example, the length of the tallest stereocilia on outer hair cells in the hamster increases gradually from 1.2 μm at the base of the cochlea to 5 μm at the apex (Kaltenbach et al., 1994). In addition, precise variations in stereocilium length are present within the highly organized staircase array of stereocilia atop each hair cell (Tilney et al., 1992) and may be required for mechanosensory transduction (Pickles and Corey, 1992).

Increases in PAB length are realized during distinct phases of development and appear to be accomplished by two different mechanisms (DeRosier and Tilney, 2000). Invertebrates rely heavily on the end-to-end joining of relatively short bundles to make long PABs of a modular design (DeRosier and Tilney, 2000). However, a modular organization has never been

Address correspondence to James R. Bartles, Dept. of Cell and Molecular Biology, Ward Building 11-185, Feinberg School of Medicine, Northwestern University, 303 East Chicago Ave., Chicago, IL 60611. Tel.: (312) 503-1545. Fax: (312) 503-7912. email: j-bartles@northwestern.edu

Key words: microvilli; stereocilia; hair cell; deafness; jerker

Abbreviations used in this paper: PAB, parallel actin bundle; CL4, LLC-PK1-CL4; CMV, cytomegalovirus; S1, myosin subfragment 1; WH2, WASP homology 2.

reported for vertebrates. This suggests that their PABs become longer principally through the further elongation of the filaments in a bundle. Little is known about how this elongation might be accomplished and what molecules might be involved.

Recent studies of GFP-actin in transfected cells support the notion that the actin filaments of PABs in the brush border microvilli of LLC-PK1-CL4 (CL4) cells (Tyska and Mooseker, 2002) and in the stereocilia of cochlear hair cells (Schneider et al., 2002) exhibit actin treadmilling. This would imply that PAB length reflects a balance between ongoing actin polymerization and depolymerization reactions in a bundle and raises the intriguing possibility that PAB length needs to be maintained throughout the life of a PAB.

We have identified and characterized espin actin-bundling proteins in the PABs of Sertoli cell junctions (Bartles et al., 1996; Chen et al., 1999), brush border microvilli of enterocytes and renal proximal tubular epithelial cells (Bartles et al., 1998), and stereocilia of hair cells in the inner ear (Zheng et al., 2000). In addition, we have determined that the espin gene is the target of the jerker deafness mutation in mice (Zheng et al., 2000). A characteristic property of the espins is that they bind to and cross-link actin filaments with a 10–100-fold higher affinity than other actin-bundling proteins ($K_d$ = 70–220 nM, depending on espin isoform; Chen et al., 1999). To determine whether espins affected PAB length and actin dynamics in PABs in vivo, we investigated the effects of espins in a well-defined model system, the brush border microvilli of CL4 cells.

## Results

Transient transfection was used to examine the effects of espins on CL4 cell microvilli and the PAB at their core. We chose transient transfection over stable transfection to facilitate comparison with untransfected neighbors. CL4 cells grown on glass coverslips formed confluent islands. After 8–10 d in culture, the cells in these islands invariably expressed uniform brush border microvilli 1–1.5 μm in length. CL4 cells derive from porcine kidney proximal tubule, and their brush border microvilli resemble their counterparts in situ by morphological, ultrastructural, and biochemical criteria (Hasson and Mooseker, 1994; Tyska and Mooseker, 2002). Consistent with the observation that espins are confined to only a subset of renal proximal tubule cells (segment S3; Bartles et al., 1998), we did not detect endogenous espins in CL4 cells by immunofluorescence or Western blotting using espin antibodies. The espin used in most of the experiments was rat Sertoli cell espin ΔN338 (Chen et al., 1999), which is missing its $NH_2$-terminal ankyrin-like repeats and coincides with the major espin isoform of cerebellar Purkinje cells (Sekerková et al., 2003). This espin was selected because it contained an optimum representation of domains, had been characterized in vitro and by transfection, was the substrate for creating a panel of mutations, and yielded two- to threefold higher levels of expression than other isoforms (see Comparison of espin isoforms…).

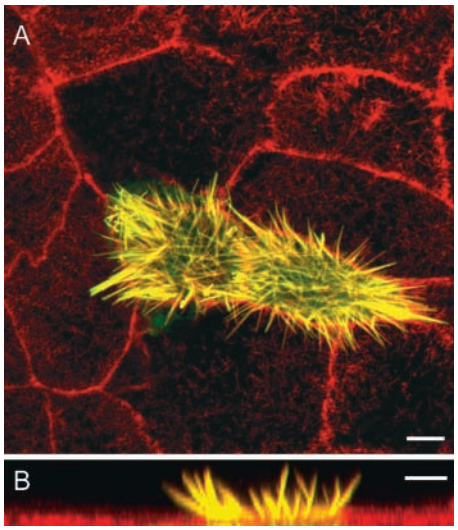


Figure 1. **Espin increases the length of microvilli in transfected CL4 cells.** CL4 cells were transfected with GFP-espin cDNA, double labeled for F-actin with Texas red–phalloidin and examined by confocal microscopy. Images of the apical surface of the monolayer are shown from (A) above or (B) the side (different fields). The GFP-espin and Texas red–phalloidin are colocalized (yellow) in microvillus-like projections that are much longer than the brush border microvilli (red) of surrounding control cells. Bars, 5 μm.

### Effect of espin on the length of CL4 cell microvilli and their PABs

After 10 d in culture, we transfected CL4 cells with a plasmid containing espin cDNA under the control of the cytomegalovirus (CMV) promoter. When transfected cells were examined 17–24 h later, the GFP-espin fusion protein was highly concentrated in the microvilli, which showed dramatic increases in length (Figs. 1 and 2). The localization of GFP-espin in the microvilli was indistinguishable from that of F-actin as revealed by double labeling with fluorescent phalloidin (Fig. 1), suggesting that the increased length of the GFP-espin–labeled microvilli mirrored a comparable increase in the length of the PAB at their core. Both fluorescent probes were distributed continuously along the length of the microvilli. Microvillar PAB length measured from oriented confocal z-sections was 7.90 ± 0.09 μm (mean ± SEM; $n$ = 555 microvilli, 28 cells) in the espin-expressing cells versus 1.33 ± 0.04 μm ($n$ = 189 microvilli, 14 cells) in neighboring untransfected control cells (Fig. 2). The GFP tag did not influence the outcome, because microvillar length increased to the same extent when espin was expressed in untagged form and localized by immunofluorescence.

EM showed that the long microvilli of espin-expressing CL4 cells were covered by plasma membrane (Fig. 3, A and B) and confirmed the presence of PABs at their core (Fig. 3, B–E). The actin filaments, which could be discerned in cross sections (Fig. 3 B), were shown to better advantage by labeling with myosin subfragment 1 (S1) after treatment with nonionic detergent (Fig. 3, C–E). Discrete bundles of actin filaments emanated from the apical surface of transfected cells and typically extended a 0.2–0.3 μm long rootlet into the apical cytoplasm (Fig. 3 E). The nonionic detergent

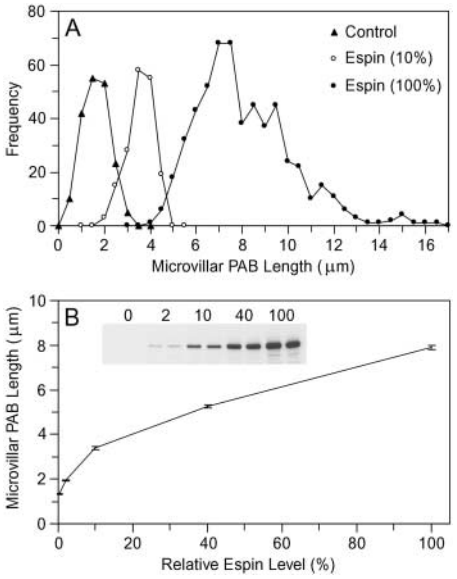


Figure 2. **Microvillar PAB length is positively correlated with espin level.** CL4 cells were transfected with GFP-espin cDNA using a series of CMV promoter deletion constructs. Microvillar PAB length was measured by confocal microscopy ($n$ = 187–555 microvilli, 12–28 cells), and replicate dishes were dissolved in SDS gel sample buffer to measure relative espin level by Western blotting (100% = full strength CMV promoter). (A) Frequency plots of microvillar PAB length for control cells and for cells transfected with two of the espin constructs. (B) Espin concentration dependence of microvillar PAB lengthening (inset, Western blot from duplicate dishes). Error bars, SEM. All groups were significant compared with control: one-way ANOVA ($F_{(4,1615)} = 1576$, $P < 0.0001$); Dunnett's test ($P < 0.01$).

treatment, which removed the plasma membrane to allow access of the S1, often caused the filaments to splay (Fig. 3 E). Nevertheless, we observed bundles of S1-decorated filaments at distances up to 5–6 μm from the apical surface (Fig. 3 C). Because of the thinness of the microvilli and the splaying, we could not trace the course of a long microvillus or its actin filaments for more than 3 μm in an ultrathin section. Nevertheless, the filaments appeared continuous in individual sections (Fig. 3, C–E). The arrowhead pattern of the S1 polar complexes was always oriented with the barbed end directed toward the microvillar tip (Fig. 3 D). Thus, the long microvilli of espin-expressing CL4 cells contained collections of actin filaments that resembled the PABs of microvilli and stereocilia in filament continuity and polarity. This suggested that these long PABs arose through elongation of the preexisting PABs found in the microvilli of control CL4 cells and not through an imperfect joining of preformed modules or through additional nucleation of actin polymerization.

## Espin concentration dependence

Qualitative comparisons of cells showing different levels of GFP-espin fluorescence on the same coverslip indicated that individual cells expressing more GFP-espin had longer microvilli. To examine the effect of espin concentration on microvillar PAB length, we performed random deletion mutagenesis of the CMV promoter and selected for analysis a group of three GFP-espin constructs that gave average GFP-espin protein expression levels that were 2, 10, and 40% of that obtained with the full-strength (wild-type) CMV promoter (100%). We measured relative protein levels by Western blotting SDS extracts prepared from replicate dishes of the transfected CL4 cells (Fig. 2 B, inset). Similar results were obtained when labeling with espin antibody or GFP antibody. No significant proteolysis of the GFP-espin was noted.

The length of the microvillar PAB was correlated positively with espin protein expression level over the range examined (Fig. 2, A and B). Significant differences from control were observed even when espin was expressed at the 2% level (1.95 ± 0.03 μm; $n$ = 197, 12 cells). Between the 10 and 100% levels, the response appeared roughly linear, a 10-fold increase in espin level resulting in an ~2.5-fold increase in length.

## Espin gradients among cochlear hair cells

We noted a similar positive correlation between espin level and stereocilium length among cochlear hair cells in situ. Cochlear hair cells exhibit a gradual approximately threefold increase in stereocilium length from base to apex along the cochlear spiral (Kaltenbach et al., 1994). We isolated cochlear whole mounts from adult rats and labeled them by immunoperoxidase or immunofluorescence using espin antibody after fixation and permeabilization with nonionic de-

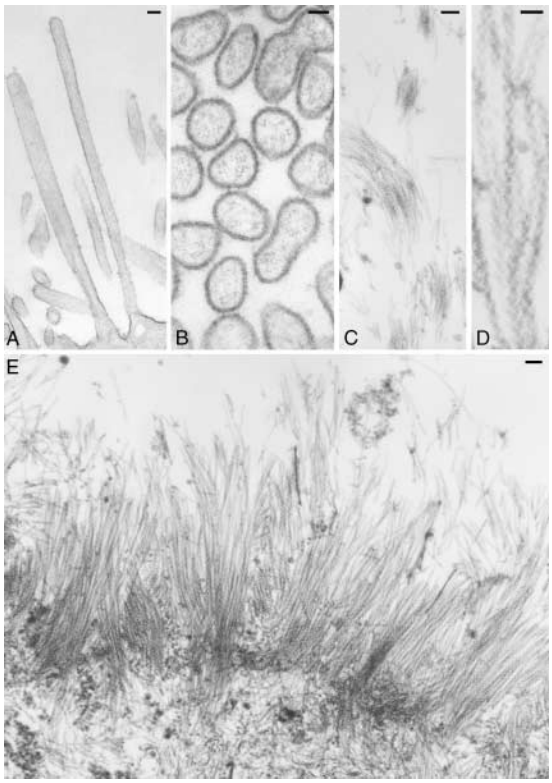


Figure 3. **The long microvilli elicited by espin contain collections of continuous actin filaments of the correct polarity.** CL4 cells were transfected with GFP-espin cDNA, fixed, and processed for EM (A and B) without or (C–E) with treatment with Triton X-100 and labeling with S1. Bars: (A, C, and E) 100 nm; (B and D) 50 nm.

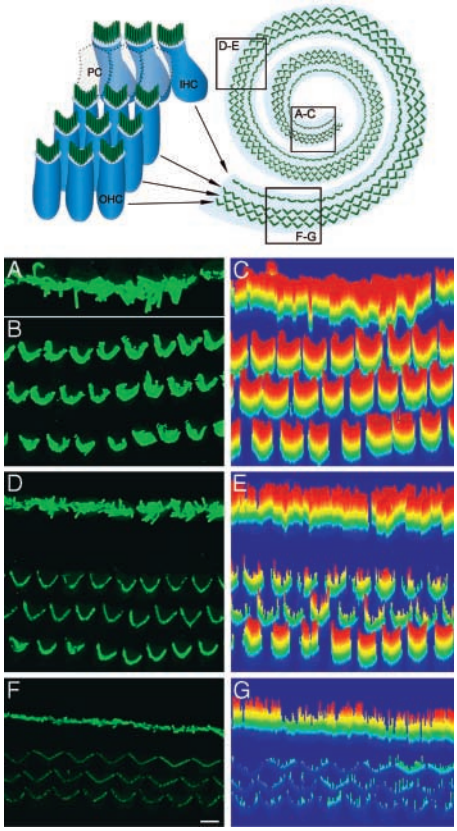


Figure 4. **Espin level is positively correlated with stereocilium length in cochlear hair cells.** (Top) Diagram of cochlear whole mount showing the three rows of outer hair cells (OHC) and one row of inner hair cells (IHC) separated by pillar cells (PC). Confocal images of hair cells in the (A and B) apical, (D) middle, and (F) basal turns of a single cochlear whole mount labeled by immunofluorescence using espin antibody were collected using identical settings. Specimen orientation dictated that the image of the inner hair cells in the (A) apical turn be collected separately from that of the (B) outer hair cells. Increases in fluorescence intensity from basal turn to apical turn are also evident in the corresponding three-dimensional color-scale intensity plots shown at the right (C, E, and G: red, high espin; blue, low espin). Bar, 5 μm.

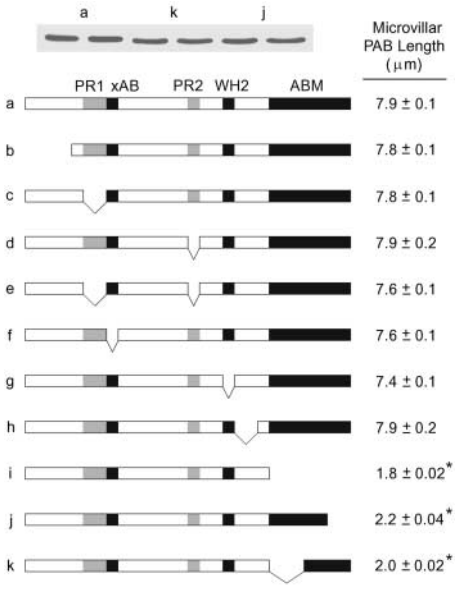


Figure 5. **The espin COOH-terminal actin-bundling module is required for PAB lengthening.** CL4 cells were transfected with the GFP-espin truncation or deletion constructs shown in the stick figure diagrams. Microvillar PAB length was measured by confocal microscopy (mean ± SEM; $n$ = 143–272 microvilli, 11–17 cells), and GFP-espin protein levels in replicate dishes were compared by Western blotting using GFP antibody (inset, sample Western blots for three constructs shown in duplicate). PR1, proline-rich peptide 1; xAB, additional F-actin–binding site; PR2, proline-rich peptide 2; WH2, WASP homology 2; ABM, actin-bundling module. ΔC117, the espin construct missing the actin-bundling module, is panel i.

tergent. With either method, we consistently observed an increasing gradient of signal intensity from base to apex along the cochlear spiral. Fig. 4 shows representative confocal images, collected using identical settings, of the apical (A and B), middle (D) and basal (F) turns of a single cochlear whole mount as depicted in the diagram (top). The endogenous espin of hair cells is concentrated in the stereocilia; for each cochlear region, a single row of inner hair cells and three rows of outer hair cells can be seen. To the right of each confocal image is a color-scale plot of fluorescence intensity (Fig. 4, C, E, and G). This exposure highlights differences in intensity among the outer hair cells from the three regions. Using estimates of fluorescence intensity computed from pixel values, the outer hair cells showed an approximately threefold average increase in fluorescence intensity from base to middle and an additional approximately threefold average increase in intensity from middle to apex.

The inner hair cells also showed an increasing gradient in espin level from base to apex along the cochlear spiral (Fig. 4, A, D, and F). At this exposure, the trend is more difficult to discern because the intensity observed for inner hair cells was greater than that of outer hair cells in each region. A difference in espin level between inner and outer hair cells may reflect different roles in signal reception versus amplification. However, this difference could also be related to inner hair cells having stereocilia that are ~1.5–2-fold longer than those of the outer hair cells, except at the extreme base of the cochlea, where they are similar in length (Kaltenbach et al., 1994).

## Espin domains involved in the lengthening effect

To identify the parts of espin required for the microvillar PAB lengthening effect, we transfected CL4 cells with truncation or deletion constructs that lacked known structural or functional domains. A number of espin domains could be eliminated without reducing lengthening, such as the proline-rich peptides (Fig. 5, c–e), the 28-aa additional F-actin–binding site (Fig. 5 f), or the WASP homology 2 (WH2) consensus domain (NSELLAEIKAGKSLKPT; Fig. 5 g). All of these mutated espin proteins were expressed at a similar level, became highly concentrated within microvilli, and increased average microvillar PAB length to 7.4–7.9 μm. The only mutations that made a major difference were those affecting the espin COOH-terminal peptide (Fig. 5, i–k, asterisks). This peptide contains the actin-bundling module that is shared among known espin isoforms and is necessary and sufficient for potent actin-bundling activity in vitro

(Bartles et al., 1998). Deletion of the actin-bundling module (ΔC117; Fig. 5 i) reduced microvillar PAB length to near control levels, even though Western blots of replicate dishes of cells transfected with espin or the ΔC117 construct showed similar levels of protein of the expected molecular mass. The ΔC117 construct did not become concentrated in microvilli, but was distributed diffusely throughout the cytoplasm. Espins, which are monomeric in solution, are believed to derive actin-bundling activity from two F-actin-binding sites disposed roughly at opposite ends of the actin-bundling module (Bartles et al., 1998; Chen et al., 1999). Consistent with a requirement for these two F-actin-binding sites, deletion of either end of the actin-bundling module also reduced microvillar PAB length to near control levels (Fig. 5, j and k) and blocked targeting to microvilli without affecting protein expression levels (Fig. 5, inset at top).

## Comparison of espin isoforms and other actin-bundling proteins

Different espin isoforms (Fig. 6 A) showed reproducible differences in level of accumulation in the transfected CL4 cells. Western blots labeled with antibody to the espin COOH-terminal peptide showed that the ~30-kD small espin (Bartles et al., 1998) and the ~110-kD espin of Sertoli cell junctions (Bartles et al., 1996) accumulated at average levels that were 30 and 60%, respectively, of that observed for the espin used in the experiments above (Fig. 6 B, top). However, when compared with the lengthening effects expected for espin when expressed at the 30 and 60% levels (interpolated from Fig. 2 B), these other espin isoforms displayed comparable lengthening activity (Fig. 6 C). The long microvilli elicited by small espin (Fig. 6 E) were generally thinner than those elicited by other espin isoforms (Fig. 6 D) and more closely resembled those of control cells in number. This suggested that domains upstream of the actin-bundling module in the larger espin isoforms (Fig. 6 A) can mediate the side-to-side bundling of microvillar PABs to yield a smaller number of thicker bundles. The COOH-terminal peptide shared by all espin isoforms (Fig. 6 A) was also expressed in CL4 cells at a lower level, similar to that of small espin (Fig. 6 B, top), and exerted a lengthening effect that was indistinguishable from that of small espin (Fig. 6 C). Thus, the COOH-terminal peptide containing the espin actin-bundling module was sufficient for the microvillar PAB lengthening effect.

We also transfected the CL4 cells with plasmids expressing other actin-bundling proteins under the control of the CMV promoter. The CL4 cells expressed GFP-tagged fascin or "constitutively active" S39A-fascin (Adams et al., 1999) at levels comparable to that of espin, as judged by Western blotting with GFP antibody (Fig. 6 B, bottom left). However, microvillar PAB length in the fascin-expressing CL4 cells was not increased significantly (Fig. 6, C and F). Instead, the fascins elicited the formation of filopodium-containing protrusions at the base of the cell, consistent with their effects on the LLC-PK1 parental line (Yamashiro et al., 1998).

GFP–T-fimbrin was expressed at an average level that was 80% of that of GFP-espin (Fig. 6 B, bottom left) and increased microvillar PAB length to 2.60 ± 0.03 μm ($n$ = 254 microvilli, 15 cells). When compared with the lengthening effect expected for GFP-espin expressed at the 80% level (Fig. 2 B), the relative microvillar PAB lengthening ac-

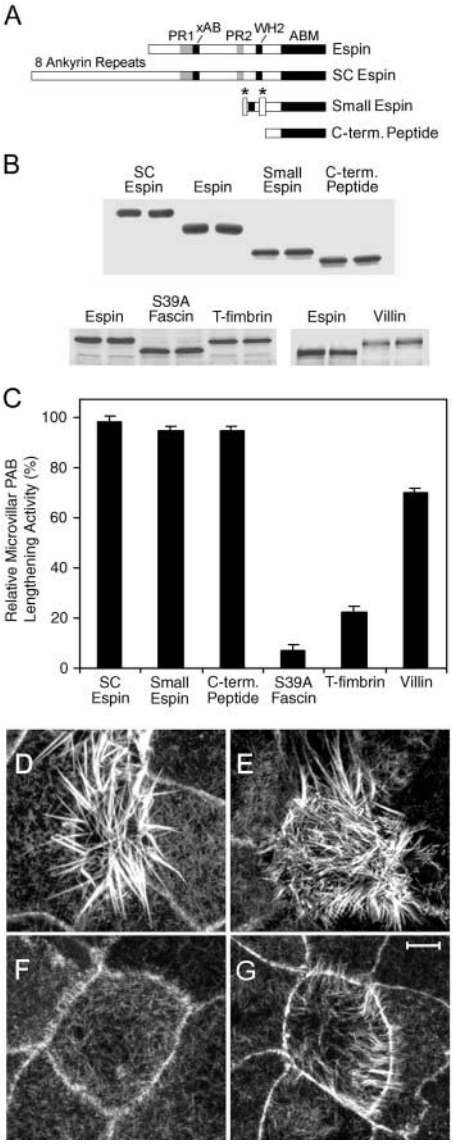


Figure 6. **Significant microvillar PAB lengthening activity is observed for espin isoforms, the espin COOH-terminal peptide, villin and T-fimbrin, but not fascin.** CL4 cells were transfected with the designated actin-bundling protein construct (SC espin, Sertoli cell espin). (A) Stick figure diagram of espin constructs. See Fig. 5 legend for domain abbreviations. Asterisks indicate peptides encoded by exons unique to small espin that bracket the WH2 domain. (B and C) Microvillar PAB length was measured by confocal microscopy, and protein levels were compared by Western blotting replicate dishes using espin COOH-terminal peptide antibody (B, top) or GFP antibody (B, bottom left and right). Length measurements were corrected for differences in level of protein accumulation using the espin concentration dependence (Fig. 2 B) and are plotted in C as a percentage of the microvillar PAB lengthening activity expected for espin when expressed at the same level (mean ± SEM; $n$ = 135–254 microvilli, 10–15 cells). All groups were significant compared with control, except S39A-fascin: one-way ANOVA ($F_{(6,1533)} = 1166$, $P < 0.0001$); Dunnett's test ($P < 0.01$). (D–G) Confocal images of the apical surface of CL4 cell monolayer showing fluorescent phalloidin localization in cells expressing (D) espin, (E) small espin, (F) S39A fascin, and (G) villin. Bar, 5 μm.

tivity of T-fimbrin was estimated to be 22% of that of espin (Fig. 6 C). CL4 cells transfected with GFP–I-fimbrin plasmid showed no differences from controls, but we could not achieve high enough levels of protein expression to allow for adequate comparison.

GFP-villin was expressed at an average level that was 30% of that of GFP-espin (Fig. 6 B, bottom right) and increased microvillar length to 3.57 ± 0.06 μm ($n$ = 197 microvilli, 13 cells). When compared with the lengthening effect expected for GFP-espin expressed at the 30% level (Fig. 2 B), the relative microvillar PAB lengthening activity of villin was estimated to be 70% of that of espin (Fig. 6 B). Similar results were obtained using GFP-tagged or untagged chicken villin and an untagged version of mouse villin. Compared with the long microvilli elicited by espin (Fig. 6 D), those formed in response to villin appeared more numerous and thin (Fig. 6 G).

## Effect of low doses of cytochalasin D

Low doses (20–200 nM) of cytochalasin D block actin polymerization by capping filament barbed ends (Sampath and Pollard, 1991), without causing the secondary effects, such as binding to monomer and nucleation of actin polymerization, that are observed at concentrations in the micromolar range (Goddette and Frieden, 1986). We compared the effects of 100 nM cytochalasin D on microvillar PAB length in transfected CL4 cells expressing small espin or espin at the 40% level. These two constructs resulted in similar levels of protein expression and increased microvillar PAB length three- to fourfold in the absence of cytochalasin D (Figs. 2 and 6). We added cytochalasin D immediately after transfection and measured microvillar PAB length 12–13 h later. The 100 nM cytochalasin D inhibited the microvillar PAB lengthening response to small espin and espin by an average of 86 ± 2% and 80 ± 2%, respectively ($n$ = 170–213 microvilli, 10–12 cells). This suggested that the espin-mediated lengthening response required additional actin polymerization predominantly, if not exclusively, at filament barbed ends. Beyond having shorter microvilli, the cells treated with 100 nM cytochalasin D showed no signs of morphological deterioration. The inhibitory effect was reversible; cells recovered long microvilli within 4.5 h after removal of the drug.

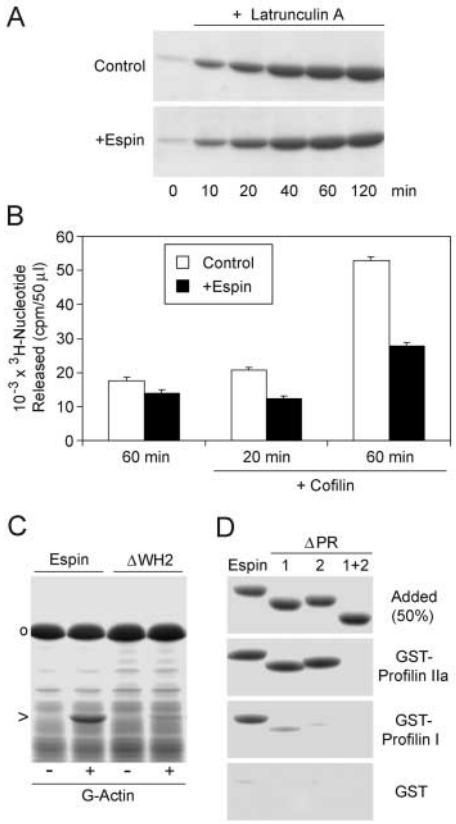


Figure 7. **Espin causes a <2-fold decrease in actin depolymerization in vitro and binds actin monomer and profilin in pull-down assays.** (A) Release of actin monomer into the supernatant after the addition of 10 μM latrunculin A to preformed actin filaments that had been incubated in the absence (Control) or presence of espin to provide a maximum level of cross-links (+Espin). (B) Release of $^3$H-nucleotide into the supernatant after the addition of an unlabeled ATP chase to actin filaments that had been polymerized in the presence of [$^3$H]ATP and incubated in the absence (Control) or presence of espin to provide a maximum level of cross-links (+Espin). In some experiments, 3 μM human cofilin was added 20 min before the unlabeled ATP (mean ± SEM; $n$ = 3). (C) Binding of G-actin to GST-espin (Espin) or GST-espin missing the WH2 consensus domain (ΔWH2) in a pull-down assay (o, GST-espin construct; >, G-actin). ~20% of the G-actin added bound to GST-espin. (D) Binding of 6X His-tagged espin constructs to GST-profilin IIa, GST-profilin I, or GST in a pull-down assay. Espin is compared with deletion constructs missing the $NH_2$-terminal (ΔPR1) or COOH-terminal (ΔPR2) proline-rich peptide or both proline-rich peptides (ΔPR1+2).

## Effect of espin on actin depolymerization in vitro

We assumed initially that espin increased PAB length because its high-affinity cross-links caused a pronounced slowing of actin depolymerization. However, in two different in vitro assays, we found that the presence of bound 6X His-tagged espin at a level predicted to achieve maximum cross-linking (approximately one espin bound/four actin monomers; Chen et al., 1999) slowed actin depolymerization <2-fold.

In one assay, we examined the rate of release of actin monomer into the high-speed supernatant as a new steady-state was approached after the addition of 10 μM of the actin monomer-sequestering drug latrunculin A to preformed filaments. Densitometric analysis of the gels showed that the presence of espin cross-links caused only a slight (≤1.3-fold) decrease in the rate of monomer release (Fig. 7 A). At the end of the experiment, ~50% of the actin monomer present initially in filaments had been released into the supernatant.

A second in vitro assay, which has been used to measure actin treadmilling rate (Carlier et al., 1997), is based on the observation that ATP/ADP bound to the actin of filaments is released only upon depolymerization from the minus end (Pollard et al., 1992). In this assay, we measured the release of $^3$H-adenine nucleotide from control or espin cross-linked filaments after initiating a "chase" with unlabeled ATP. The presence of espin cross-links reduced nucleotide release 1.3-fold at 60 min (Fig. 7 B). The addition of 3 μM cofilin increased the rate of nucleotide release approximately threefold in the absence of espin (Fig. 7 B). In the presence of cofilin, the espin cross-links had a slightly larger effect, decreasing

nucleotide release 1.7- and 1.9-fold at 20 and 60 min, respectively (Fig. 7 B).

### Effect of espin on treadmilling in microvillar PABs: identification of actin monomer-binding and profilin-binding domains

Next, we used FRAP to determine whether espin affected treadmilling dynamics in the long microvillar PABs of espin-expressing CL4 cells. Cells were cotransfected with plasmids encoding untagged espin and GFP–β-actin. The expression of the GFP–β-actin had no effect on microvillar PAB length when expressed in the absence of espin. In initial experiments, we could find examples of a rapid recovery of GFP–β-actin fluorescence at the tip of photobleached long microvilli. However, an unexpectedly rapid recovery of GFP–β-actin fluorescence throughout the entire microvillus frequently obscured the site of initial recovery and consistently precluded efforts to monitor any subsequent tip to base movements of the zone of recovered GFP–β-actin fluorescence (Fig. 8 A).

The rapid recovery throughout the long microvilli appeared to be attributable to the binding of actin monomer and profilin–actin complex to espin in the microvilli. In pull-down assays, GST-espin fusion protein bound G-actin, and the binding was reduced to near background levels (approximately eightfold) by deletion of the WH2 domain (Fig. 7 C). This suggested that G-actin did not bind well to the F-actin binding sites in the COOH-terminal actin-bundling module or the additional F-actin–binding site (Fig. 5 a, diagram; Bartles et al., 1998; Chen et al., 1999). Similar results were obtained when the pull-down assay was performed in the presence of 10 μM latrunculin A to ensure that the actin remained monomeric. In other pull-down assays, 6× His-tagged espin bound to GST-profilin IIa or GST-profilin I, and this binding was eliminated by deletion of the espin proline-rich peptides (Fig. 7 D). We established empirically that deletion of two espin domains, the eight-proline stretch in the COOH-terminal proline-rich peptide and the WH2 domain ($\Delta P_8\Delta$WH2), dramatically reduced the tendency of GFP–β-actin fluorescence to rapidly recover along the entire microvillus in FRAP. However, this combination of deletions did not decrease microvillar PAB lengthening activity (microvillar PAB length, 8.0 ± 0.1 μm [$n$ = 152 microvilli, 16 cells] compare with Fig. 5, right column).

CL4 cells were examined by FRAP either 4 h or 24 h after cotransfection with GFP–β-actin and untagged $\Delta P_8\Delta$WH2 espin constructs. The microvilli examined at 4 h were selected to be of intermediate length (2.5–4.5 μm) to increase the likelihood that they were undergoing lengthening at the time of observation. Whether examined at 4 or 24 h, photobleached microvilli consistently showed a rapid (1–2 min) recovery of GFP–β-actin fluorescence at their tips (Fig. 8 B). On the basis of the polarity of the filaments (Fig. 3), this was the location expected for filament barbed ends. The conclusion that filament barbed ends were concentrated at the microvillar tip and not elsewhere in the long microvillar PABs was supported by the pattern of rhodamine-actin incorporation observed in detergent-permeabilized cells. Rhodamine-actin fluorescence was highly concentrated at microvillar tips whether cells were labeled 4 h (Fig. 8, D and E) or 24 h (Fig. 8, F and G) after transfection with the $\Delta P_8\Delta$WH2 espin construct.

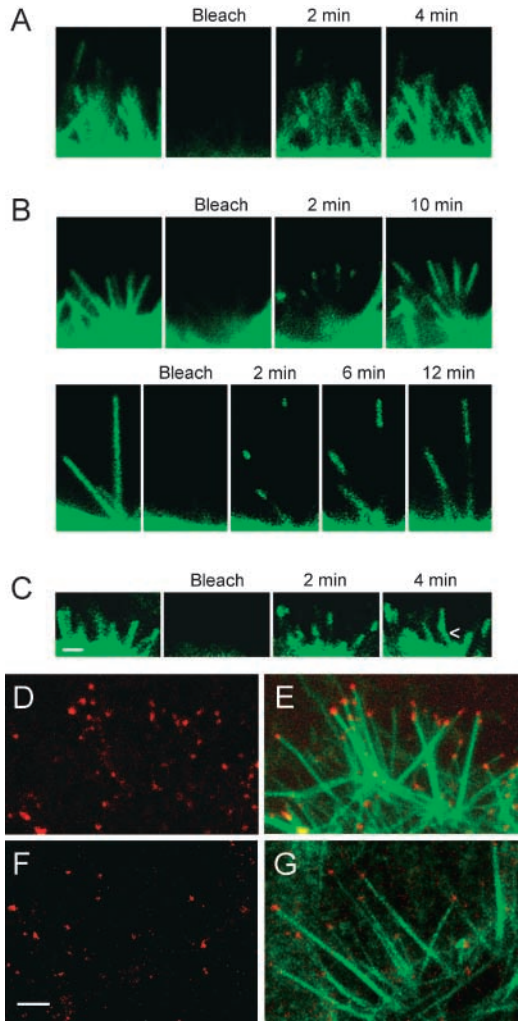


Figure 8. **FRAP and rhodamine-actin decoration reveal actin incorporation at the microvillar tip and actin treadmilling in the long microvilli of espin-expressing CL4 cells.** (A–C) Examples of GFP–β-actin FRAP in microvilli of CL4 cells expressing espin (A), the $\Delta P_8\Delta$WH2 espin construct (B), or no espin (C). Recovery times are shown. Arrowhead in C represents a microvillus as it enters field and obscures recovery. Bar, 1 μm. (D–G) Rhodamine-actin labeling in the microvilli of detergent-permeabilized CL4 cells (D and E) 4 h or (F and G) 24 h after transfection with the $\Delta P_8\Delta$WH2 espin construct (E and G, with fluorescein-phalloidin counterstain). Bar, 2 μm.

After the rapid recovery of GFP–β-actin fluorescence at the microvillar tip, the size of the recovered zone increased by extension toward the base of the microvillus at a relatively constant rate (Fig. 8 B), presumably because of actin treadmilling in the long microvillar PABs (Schneider et al., 2002; Tyska and Mooseker, 2002). The long microvilli frequently changed positions during monitoring and became obscured by other microvilli. This made it difficult to follow the extension of the zone of recovered fluorescence more than halfway down the microvillus. From measurements made at 2-min intervals during the first 6–10 min of recovery, the rates of movement of the recovered zone were 0.27 ± 0.01 μm/min (mean ± SEM; $n$ = 138 microvilli, 20 cells) and 0.24 ± 0.01 μm/min ($n$ = 105 microvilli, 17 cells) for microvilli ex-

amined 4 and 24 h after transfection, respectively. Assuming a rise per actin subunit of 2.75 nm in the F-actin helix, this suggested that the microvillar PABs in espin-expressing cells were undergoing actin treadmilling at a similar rate, 1.5–1.6 (actin subunits) $s^{-1}$, during and after elongation.

We also examined the rate of actin treadmilling in the short microvilli of control cells 24 h after transfection with the GFP–β-actin construct alone. The higher density of microvilli on control cells necessitated that the FRAP analysis be confined to subsets of microvilli in relative isolation near the edge of a given collection that were, because of irregularities in the monolayer, tipped more parallel to the substratum (Fig. 8 C). In addition, the shortness of the control microvilli reduced the number of time points that could be examined. For observations made during the first 4–6 min of recovery, the rate of movement of the recovered zone in the microvilli of control cells was 0.21 ± 0.01 μm/min ($n$ = 143 microvilli, 19 cells), corresponding to an actin treadmilling rate of 1.3 $s^{-1}$. Thus, espin did not slow actin treadmilling in microvillar PABs, but actually appeared to cause a slight increase.

## Discussion

We have uncovered a mechanism by which cells can use a specific class of actin-bundling protein, the espins, to make longer microvillus-type PABs without needing to join shorter PAB modules. This activity, which appears to stem from an ability of espin cross-links to effect a net barbed-end elongation of the treadmilling actin filaments in these PABs, distinguishes espins from at least two other classes of actin-bundling protein and may explain the shortening of hair cell stereocilia observed in the espin-deficient jerker mouse.

### More espin, longer PABs

The espins exerted a reproducible, concentration-dependent lengthening effect on the microvillar PABs of CL4 epithelial cells and could, presumably, have a lengthening effect on microvillus-type PABs in other cells, including the stereocilia of hair cells. At the highest espin level examined, microvillar PAB length increased an average of sixfold, but in extreme examples increased 13-fold. Significant 1.5- and 2.5-fold increases in length were observed at 2 and 10% of this maximum espin level, suggesting that supraphysiological levels are not required to observe an effect. Accordingly, the average lengths attained at the 2% (2.0 μm), 10% (3.4 μm), 40% (5.3 μm), and 100% (7.9 μm) espin levels span the range of lengths observed for the microvilli and stereocilia of most mammalian cells. Moreover, a similar correlation, in which a 9–10-fold increase in espin level is associated with a 2.5–3-fold increase in PAB length, was noted for the microvillar PABs of CL4 cells and the stereocilia of cochlear hair cells in situ.

### Different actin-bundling proteins, different effects

Our results provide an illustration of how, in the same cell, different actin-bundling proteins become associated with, and exert their effects on, different classes of PAB-containing structures. Although espins became concentrated in the microvillar PABs and increased their length, fascin became concentrated in filopodium-like elements of protrusions that it caused to extend from the opposite end of the cell. This is consistent with the role proposed for fascin in the formation of filopodia (Svitkina et al., 2003) and suggests that the PABs of microvilli and filopodia differ qualitatively. The fimbrins are believed to contribute cross-links to the PABs of brush border microvilli and hair cell stereocilia (Mooseker, 1985; Tilney et al., 1989), and T-fimbrin accumulates in stereocilia during stereociliogenesis (Daudet and Lebart, 2002). Although T-fimbrin has been reported to cause some increases in microvillar dimensions in the LLC-PK1 parental line (Arpin et al., 1994), it was less active than the espins at increasing microvillar PAB length in CL4 cells. We uncovered an unanticipated functional similarity between espins and villin in their ability to increase the length of CL4 cell microvillar PABs. Our findings reinforce earlier work showing that villin can induce microvilli in transfected or microinjected cells (Franck et al., 1990; Friederich et al., 1992; Arpin et al., 1994) and are consistent with a role for villin in remodeling the enterocyte brush border after damage (Ferrary et al., 1999).

### Elongation of existing microvillar PABs

Our results suggest that espins increase PAB length by causing a net barbed-end elongation of the treadmilling actin filaments that exist within the relatively short microvillar PABs of control CL4 cells before espin expression. Key support comes from the observation that the actin filaments of the long microvillar PABs in espin-expressing cells appear continuous from rootlet to tip. Although this continuity could arise secondarily, through additional nucleation events followed by a stitching together of loose ends, we saw no instances of bundle discontinuity, and the site of fluorescent actin incorporation (barbed ends) remained concentrated at the microvillar tip during and after lengthening. The existence of actin treadmilling in the long microvillar PABs, which we detected by FRAP, is further evidence in support of filament continuity. Also consistent with a mechanism involving the elongation of existing microvillar PABs is the inverse correlation we noted between microvillus number and thickness. Small espin tended to make microvilli that were relatively thin and more comparable in number to those found on control cells, whereas the larger espin isoforms made a smaller number of thicker microvilli. Thus, in addition to causing PAB elongation, the larger espin isoforms appear to cross-link the existing microvillar PABs to yield a smaller number of thicker microvilli. Finally, although we discovered that espins contain two types of functional domains commonly found in proteins involved in the nucleation of actin polymerization, namely an actin monomer-binding WH2 domain (Welch and Mullins, 2002) and profilin-binding proline-rich peptides (Evangelista et al., 2003), these two domains appear not to be required for PAB lengthening and are presumably required in other contexts. The net barbed-end elongation of treadmilling actin filaments in microvillar PABs mediated by espins may be one way that vertebrate cells make PABs longer without having to join bundle modules. Obvious espin orthologues are present in vertebrates from *Fugu* to human.

### Effects of espins on actin polymerization/depolymerization reactions in PABs

The espin COOH-terminal peptide, which contains the actin-bundling module, was necessary and sufficient for the microvillar PAB-lengthening effect. Moreover, lengthening required the two putative F-actin–binding sites disposed at opposite ends of the actin-bundling module. Thus, lengthening is likely attributable to espin cross-links. In view of espin's high affinity for binding and cross-linking F-actin in vitro (Chen et al., 1999), we were surprised that the microvillar PABs of the espin-expressing CL4 cells appeared to undergo actin treadmilling at a similar rate to those in control cells without espin. However, this was consistent with the modest effect of espin cross-links on actin depolymerization and treadmilling in vitro. Because espin can bind G-actin via its WH2 domain, the 1.3–1.9-fold decreases noted in the in vitro assays may actually be overestimates.

The rate of actin treadmilling we observed in the microvillar PABs of transiently transfected CL4 cells was $\sim$1.5 $s^{-1}$. This is five times faster than the rate calculated by Tyska and Mooseker (2002) for the microvilli of control CL4 cells stably expressing GFP–β-actin and closer to the rate in their partially differentiated cells ($\sim$3 $s^{-1}$). It is also $\sim$20 and $\sim$150 times faster than the actin treadmilling reported for the stereocilia of transfected hair cells in cochlear explants isolated from postnatal day one to three rats and maintained in culture for 3–5 d or 10–15 d, respectively (Schneider et al., 2002). Although 1.5 $s^{-1}$ may be relatively fast for actin treadmilling in a microvillus-type PAB, it is 2.5 times slower than the average rate in stationary filopodia (Mallavarapu and Mitchison, 1999), and $\sim$5–50 times slower than the rates of actin filament turnover attained in the lamellipodia of migrating cells or in *Listeria* comet tails (for review see Pollard and Borisy, 2003).

The observation that the microvillar PABs of CL4 cells undergo actin treadmilling at $\sim$1.5 $s^{-1}$ in the absence or presence of espin implies that espin cross-links cause PAB elongation through relatively subtle effects on the rates of actin polymerization and/or depolymerization. For example, when treadmilling is 1.5 $s^{-1}$ (0.24 μm/min), the elongation of a PAB from 1.3 to 7.9 μm can be accomplished in 55 min by a transient twofold decrease in the rate of actin depolymerization at filament pointed ends or in 27.5 min by a transient twofold increase in the rate of actin polymerization at filament barbed ends. If 4 h are allotted, then elongation from 1.3 to 7.9 μm can be accomplished by a transient change in the rate of actin polymerization or depolymerization of $\sim$10%. Changes of such a small magnitude would be difficult to detect using in vitro assays and may depend on the contributions of other cellular proteins. Although the slight increase in actin treadmilling rate apparent in espin-expressing cells may be indicative of a subtle effect of espin on actin dynamics, an increase in treadmilling rate alone would be insufficient to cause lengthening.

### Implications for the jerker phenotype

The microvillar PABs of espin-expressing cells do not elongate indefinitely, which suggests that the system regulates naturally to a steady-state. Moreover, the PABs continue to undergo actin treadmilling at $\sim$1.5 $s^{-1}$ after reaching a steady-state length. Thus, the positive correlation between espin level and steady-state microvillar PAB length suggests that specific numbers of espin cross-links must remain present to balance actin depolymerization from filament pointed ends and maintain a stable length for the PAB. A requirement for espin to maintain the steady-state length of a treadmilling PAB could explain the shortening of hair cell stereocilia observed in homozygous jerker mice. The hair cells of these mice, which are deficient in espin protein because of a frameshift mutation in the espin gene (Zheng et al., 2000), have been reported to sprout and organize collections of stereocilia that appear relatively normal (Sjöström and Anniko, 1992). Although there has not yet been a quantitative analysis of stereocilium length in these mice, this suggests that espins are not required to establish a basic stereociliary array. Around postnatal day 10, the stereocilia of cochlear hair cells begin to collapse, shorten, and disappear in jerker homozygotes (Sjöström and Anniko, 1992). We hypothesize that around postnatal day 10 the PABs of stereocilia enter a new life-cycle phase characterized by faster actin treadmilling. This could reflect a physiological activation of the hair cell and might afford greater responsiveness to stimuli or facilitate repair. We propose that it is during this more dynamic phase that specific numbers of espin cross-links become necessary to balance a faster rate of actin depolymerization from filament pointed ends and maintain a fixed steady-state length for each stereocilium. On the basis of the weak activity of T-fimbrin in the microvillar PAB lengthening assay, the fimbrins of the stereocilium may not be able to compensate for the lack of espins. The seemingly stable and precise variations in PAB length maintained in the staircase array of stereocilia on each hair cell suggests that there may be mechanisms to compartmentalize and/or regulate espins locally within the hair cell.

## Materials and methods

The following materials were obtained from the designated sources: CL4 cells (M. Tyska and M. Mooseker, Yale University, New Haven, CT); human fascin and S39A fascin plasmids (D. Vignjevic and G.G. Borisy, Northwestern University, Chicago, IL); chicken villin and human fimbrin plasmids (P. Matsudaira, Whitehead Institute, Cambridge, MA); S1 (R.D. Goldman, Northwestern University, Chicago, IL); mouse villin plasmid (American Type Culture Collection); rabbit skeletal muscle actin, rhodamine-actin and human cofilin (Cytoskeleton Inc.); and Lipofectamine and cell culture supplies (Invitrogen). Expression constructs were in the pEGFP-C (BD Biosciences) or pcDNA3 (Invitrogen) vector. Espin cDNAs with mutations were prepared using restriction sites or PCR and checked by sequence analysis. CMV promoter mutagenesis was as described previously (Watanabe and Mitchison, 2002). Rat profilin I and IIa cDNAs were prepared from rat brain by RT-PCR and expressed in *E. coli* BL21 Star (DE3; Invitrogen) as GST fusion proteins (pGEX-4T-2 vector; Amersham Biosciences). Espin proteins were expressed with an $NH_2$-terminal 6X His tag (Sekerková et al., 2003) or as GST fusion proteins.

CL4 cells were cultured at 37°C in minimum essential medium alpha medium (with L-glutamine, without nucleosides) supplemented with 10% FBS and 100 U/ml penicillin and streptomycin. Cells cultured on glass coverslips for 10 d ($\sim$75% confluency) were transfected for 4 h with a fixed amount of plasmid DNA using Lipofectamine (Chen et al., 1999) and examined 17–24 h later. In some experiments, cytochalasin D (Sigma-Aldrich) was added after transfection from a 1,000-fold concentrated stock in DMSO. CL4 cells were fixed with PFA, treated briefly with 0.1% Triton X-100, labeled with antibodies and/or Texas red–phalloidin (Molecular

Probes) to detect F-actin, and mounted in 5% (wt/vol) *n*-propylgallate, 90% (vol/vol) glycerol (Chen et al., 1999). Transfected cells were identified by GFP fluorescence or, for untagged constructs or GFP constructs of low promoter strength, by immunofluorescence using the following antibodies with Alexa 488–goat secondary antibodies (Molecular Probes): affinity purified rabbit polyclonal anti–rat Purkinje cell espin 1 (Sekerková et al., 2003), anti–rat espin COOH-terminal peptide (Zheng et al., 2000), mouse monoclonal anti-GFP (Roche), or antivillin (Immunotech). Cochlear whole mounts, obtained by dissection (Sobkowicz et al., 1993) of EDTA-decalcified bony labyrinths from PFA-fixed adult rats (Zheng et al., 2000), were labeled with affinity purified espin antibody and Alexa 488–goat anti–rabbit secondary antibody and mounted in Vectashield (Vector) or labeled by the ABC immunoperoxidase procedure (Zheng et al., 2000).

0.5-μm confocal z-sections were collected at RT using a confocal microscope (model LSM 510 META; Carl Zeiss MicroImaging, Inc.) and a 100X, 1.4 NA oil immersion objective. LSM510 imaging software was used to generate orthogonal sections, from which measurements of microvillar length were made on cells selected at random from the ~30–40% of transfected cells that showed similar high levels of expression. Microvillar length measurements were made on those for which a complete course could be charted. Significance was evaluated by one-way ANOVA and confirmed using Dunnett's post-hoc test. Z-section images of hair cells from basal, middle, and apical turns of individual cochleas were collected using identical settings. Average intensity values for individual hair cells were measured from digitized confocal images using Metamorph (Universal Imaging Corp.). Images were saved in TIF format, transferred to Photoshop (Adobe Systems), assembled into composites and converted to CMYK color format with minor adjustments of brightness and contrast. CL4 cells were processed for EM without (Tilney et al., 1998) or with labeling with S1 (Svitkina and Borisy, 1998) and examined using an electron microscope (model JEM-1200 EX; JEOL). FRAP (Yoon et al., 1998) was performed on cells cotransfected with pEGFP-C–β-actin and pcDNA3 espin or $\Delta P_8\Delta$WH2 espin. Filament barbed ends were localized by incorporation of rhodamine-actin after detergent permeabilization (Symons and Mitchison, 1991).

Western blotting was performed on hot SDS gel sample buffer extracts of replicate dishes of transfected cells using the ECL method (Amersham Biosciences). Rabbit skeletal muscle actin was polymerized and incubated with or without 6X His-tagged espin as described previously (Chen et al., 1999). 10 μM latrunculin A was added, and supernatants were collected by centrifugation for 20 min at 164,000 *g* in an ultracentrifuge (model TLA100.3 rotor/TL-100; Beckman Coulter) and analyzed in Coomassie blue–stained SDS gels. Actin depolymerization/treadmilling was assayed using the sedimentation version of the method of Carlier et al. (1997), in which [2,8-$^3$H]ATP (Amersham Biosciences) was substituted for fluorescent ATP analogue. The chase with unlabeled ATP was started 60 min after adding 6X His-tagged espin or buffer. Supernatants were collected by centrifugation (see above), and the released $^3$H-adenine nucleotide was measured in a scintillation counter. In some experiments, 3 μM human cofilin was added 20 min before the chase. GST pull-down assays were conducted as described using either 6X His-tagged espin constructs (Sekerková et al., 2003) or G-actin (Uruno et al., 2001) as ligand.

We thank M. Tyska and M. Mooseker for the CL4 cells; D. Vignjevic and G. Borisy for fascin plasmids; P. Matsudaira for fimbrin and chicken villin plasmids; R. Goldman for S1; T. Svitkina for advice about S1; and K. Myung and L. Reynolds for specimen processing and sectioning.

This work used the confocal in the Northwestern University Cell Imaging Facility. We are especially indebted to B. Fritsch and K. Beisel for suggesting that we search for differences in espin protein level among hair cells. This work was supported by grant DC004314 to J.R. Bartles from the National Institute on Deafness and Other Communication Disorders.

Submitted: 15 September 2003
Accepted: 27 October 2003

# References

Adams, J.C., J.D. Clelland, G.D. Collett, F. Matsumura, S. Yamashiro, and L. Zhang. 1999. Cell-matrix adhesions differentially regulate fascin phosphorylation. *Mol. Biol. Cell.* 10:4177–4190.

Arpin, M., E. Friederich, M. Algrain, F. Vernel, and D. Louvard. 1994. Functional differences between L- and T-plastin isoforms. *J. Cell Biol.* 127:1995–2008.

Bartles, J.R. 2000. Parallel actin bundles and their multiple actin-bundling proteins. *Curr. Opin. Cell Biol.* 12:72–78.

Bartles, J.R., A. Wierda, and L. Zheng. 1996. Identification and characterization of espin, an actin-binding protein localized to the F-actin-rich junctional plaques of Sertoli cell ectoplasmic specializations. *J. Cell Sci.* 109:1229–1239.

Bartles, J.R., L. Zheng, A. Li, A. Wierda, and B. Chen. 1998. Small espin: a third actin-bundling protein and potential forked protein ortholog in brush border microvilli. *J. Cell Biol.* 143:107–119.

Carlier, M.F., V. Laurent, J. Santolini, R. Melki, D. Didry, G.X. Xia, Y. Hong, N.H. Chua, and D. Pantaloni. 1997. Actin depolymerizing factor (ADF/cofilin) enhances the rate of actin filament turnover: implication in actin-based motility. *J. Cell Biol.* 136:1307–1322.

Chen, B., A. Li, D. Wang, M. Wang, L. Zheng, and J.R. Bartles. 1999. Espin contains an addition actin-binding site in its N terminus and is a major actin-bundling protein of the Sertoli cell-spermatid ectoplasmic specialization junctional plaque. *Mol. Biol. Cell.* 10:4327–4339.

Daudet, N., and M.-C. Lebart. 2002. Transient expression of the T-isoform of plastins/fimbrin in the stereocilia of developing auditory hair cells. *Cell Motil. Cytoskeleton.* 53:326–336.

DeRosier, D.J., and L.G. Tilney. 2000. F-actin bundles are derivatives of microvilli: what does this tell us about how bundles might form? *J. Cell Biol.* 148:1–6.

Evangelista, M., S. Zigmond, and C. Boone. 2003. Formins: signaling effectors for assembly and polarization of actin filaments. *J. Cell Sci.* 116:2603–2611.

Ferrary, E., M. Cohen-Tannoudji, G. Pehau-Arnaudet, A. Lapillonne, R. Athman, T. Ruiz, L. Boulouha, F. El Marjou, A. Doye, J.J. Fontaine, et al. 1999. In vivo, villin is required for $Ca^{2+}$-dependent F-actin disruption in intestinal brush borders. *J. Cell Biol.* 146:819–830.

Franck, Z., M. Footer, and A. Bretscher. 1990. Microinjection of villin into cultured cells induces rapid and long-lasting changes in cell morphology but does not inhibit cytokinesis, cell motility, or membrane ruffling. *J. Cell Biol.* 111:2475–2485.

Friederich, E., K. Vancompernolle, C. Huet, M. Goethals, J. Finidori, J. Vandekerckhove, and D. Louvard. 1992. An actin-binding site containing a conserved motif of charged amino acid residues is essential for the morphogenetic effect of villin. *Cell.* 70:81–92.

Goddette, D.W., and C. Frieden. 1986. Actin polymerization. The mechanism of action of cytochalasin D. *J. Biol. Chem.* 261:15974–15980.

Hasson, T., and M.S. Mooseker. 1994. Porcine myosin VI: characterization of a new mammalian unconventional myosin. *J. Cell Biol.* 127:425–440.

Kaltenbach, J.A., P.R. Falzarano, and T.H. Simpson. 1994. Postnatal development of the hamster cochlea. II. Growth and differentiation of stereocilia bundles. *J. Comp. Neurol.* 350:187–198.

Mallavarapu, A., and T. Mitchison. 1999. Regulated actin cytoskeleton assembly at filopodium tips controls their extension and retraction. *J. Cell Biol.* 146: 1097–1106.

Mooseker, M.S. 1985. Organization, chemistry, and assembly of the cytoskeletal apparatus of the intestinal brush border. *Annu. Rev. Cell Biol.* 1:209–241.

Pacini, P., G.E. Orlandini, and A.F. Holstein. 1980. Scanning electron microscopy of the human male genital tract. *Bull. Assoc. Anat. (Nancy).* 64:561–566.

Pickles, J.O., and D.P. Corey. 1992. Mechanoelectrical transduction by hair cells. *Trends Neurosci.* 15:254–259.

Pollard, T.D., and G.G. Borisy. 2003. Cellular motility driven by assembly and disassembly of actin filaments. *Cell.* 112:453–465.

Pollard, T.D., I. Goldberg, and W.H. Schwarz. 1992. Nucleotide exchange, structure and mechanical properties of filaments assembled from ATP-actin and ADP-actin. *J. Biol. Chem.* 267:20339–20345.

Sampath, P., and T.D. Pollard. 1991. Effects of cytochalasin, phalloidin, and pH on the elongation of actin filaments. *Biochemistry.* 30:1973–1980.

Schneider, M.E., I.A. Belyantseva, R.B. Azevedo, and B. Kachar. 2002. Rapid renewal of auditory hair bundles. *Nature.* 418:837–838.

Sekerková, G., P.A. Loomis, B. Changyaleket, L. Zheng, R. Eytan, B. Chen, E. Mugnaini, and J.R. Bartles. 2003. Novel espin actin-bundling proteins are localized to Purkinje cell dendritic spines and bind the Src homology 3 adapter protein insulin receptor substrate p53. *J. Neurosci.* 23:1310–1319.

Sjöström, B., and M. Anniko. 1992. Genetically induced inner ear degeneration. A structural and functional study. *Acta Otolaryngol. Suppl.* 493:141–146.

Sobkowicz, H.M., J.M. Loftus, and S.M. Slapnick. 1993. Tissue culture of the organ of Corti. *Acta Otolaryngol. Suppl.* 502:3–36.

Svitkina, T.M., and G.G. Borisy. 1998. Correlative light and electron microscopy of the cytoskeleton of cultured cells. *Methods Enzymol.* 298:570–592.

Svitkina, T.M., E.A. Bulanova, O.Y. Chaga, D.M. Vignjevic, S. Kojima, J.M. Vasiliev, and G.G. Borisy. 2003. Mechanism of filopodia initiation by reorga-

nization of a dendritic network. *J. Cell Biol.* 160:409–421.

Symons, M.H., and T.J. Mitchison. 1991. Control of actin polymerization in live and permeabilized fibroblasts. *J. Cell Biol.* 114:503–513.

Tilney, L.G., M.S. Tilney, and D.J. DeRosier. 1992. Actin filaments, stereocilia and hair cells: how cells count and measure. *Annu. Rev. Cell Biol.* 8:257–274.

Tilney, L.G., P.S. Connelly, K.A. Vranich, M.K. Shaw, and G.M. Guild. 1998. Why are two different cross-linkers necessary for actin bundle formation in vivo and what does each cross-link contribute. *J. Cell Biol.* 143:121–133.

Tilney, M.S., L.G. Tilney, R.E. Stephens, C. Merte, D. Drenckhahn, D.A. Cotanche, and A. Bretscher. 1989. Preliminary characterization of the stereocilia and cuticular plate of hair cells in the chick cochlea. *J. Cell Biol.* 109: 1711–1723.

Tyska, M.J., and M.S. Mooseker. 2002. MYO1A (brush border myosin I) dynamics in the brush border of LLC-PK1-CL4 cells. *Biophys. J.* 82:1869–1883.

Uruno, T., J. Liu, P. Zhang, Y. Fan, C. Egile, R. Li, S.C. Mueller, and X. Zhan. 2001. Activation of Arp2/3 complex-mediated actin polymerization by cortactin. *Nat. Cell Biol.* 3:259–266.

Watanabe, N., and T.J. Mitchison. 2002. Single-molecule speckle analysis of actin filament turnover in lamellipodia. *Science.* 295:1083–1086.

Welch, M.D., and R.D. Mullins. 2002. Cellular control of actin nucleation. *Annu. Rev. Cell Dev. Biol.* 18:247–288.

Yamashiro, S., Y. Yamakita, S. Ono, and F. Matsumura. 1998. Fascin, an actin-bundling protein, induces membrane protrusions and increases cell motility of epithelial cells. *Mol. Biol. Cell.* 9:993–1006.

Yoon, M., R.D. Moir, V. Prahlad, and R.D. Goldman. 1998. Motile properties of vimentin intermediate filament networks in living cells. *J. Cell Biol.* 143: 147–157.

Zheng, L., G. Sekerková, K. Vranich, L.G. Tilney, E. Mugnaini, and J.R. Bartles. 2000. The deaf jerker mouse has a mutation in the gene encoding the espin actin-bundling proteins of hair cell stereocilia and lacks espins. *Cell.* 102: 377–385.